

# The preliminary study of diabetic retinopathy detection based on intensity parameters with optical coherence tomography angiography

J.Hou<sup>1</sup>, H.Shi<sup>1</sup>, W.Gao<sup>2</sup>, P.Lin<sup>3</sup>, B.Li<sup>3</sup>, Y.Shi<sup>3</sup>, I.A.Matveeva<sup>4</sup>, V.P.Zakharov<sup>4</sup>, I.A.Bratchenko<sup>4</sup>

<sup>1</sup> School of Safety Engineering, Ningbo University of Technology,  
China, Zhejiang, Ningbo, Jiangbei, Fenghua Rd. 201;

<sup>2</sup> School of Computer Science, Ningbo University of Technology,  
China, Zhejiang, Ningbo, Jiangbei, Fenghua Rd. 201;

<sup>3</sup> Department of Ophthalmology, Ningbo First Hospital,  
China, Zhejiang, Ningbo, Haishu, Liuting St. 59;

<sup>4</sup> Department of Laser and Biotechnical Systems, Samara National Research University,  
443086, Russia, Samara, Lukacheva St. 39B

## Abstract

In this study, the diagnostic abilities of intensity parameters of optical coherence tomography angiography (OCTA) images in the early detection of diabetic retinopathy (DR) were determined. 78 normal healthy eyes, 10 diabetic eyes with mild non-proliferative diabetic retinopathy (NPDR), and 10 diabetic eyes with moderate NPDR were employed. Four retinal vascular plexuses were generated by using OCTA, which included the nerve fiber layer vascular plexus (NFLVP), superficial vascular plexus (SVP), intermediate capillary plexus (ICP) and deep capillary plexus (DCP). The parafoveal zone in each OCTA image was divided into four sectors which were the superior, temporal, inferior, and nasal sectors. Five intensity parameters including the mean, median, variance, skewness, and kurtosis of intensities were calculated for each sector. The factor of aging was evaluated among normal healthy subgroups. The diagnostic abilities of intensity parameters were evaluated between normal healthy subjects and diabetic patients with DR. Our results showed that the variance of intensities in superior sector in ICP achieved the highest AUROC value of 0.95 with the sensitivity of 0.87 and the specificity of 1.000 when comparing the diabetic patients with the mild NPDR to normal healthy subjects. The mean intensity in superior sector in ICP achieved the second highest AUROC value of 0.95 with the sensitivity of 0.90 and the specificity of 0.90 when comparing the diabetic patients with the moderate NPDR to normal healthy subjects. The proposed approach could offer a simple way to differentiate diabetic patients with early DR from normal healthy subjects without performing the relatively complicated image processing techniques.

**Keywords:** diabetic retinopathy, optical coherence tomography angiography, intensity, variance.

**Citation:** Hou J, Shi H, Gao W, Lin P, Li B, Shi Y, Matveeva I, Zakharov V, Bratchenko I. The preliminary study of diabetic retinopathy detection based on intensity parameters with optical coherence tomography angiography. *Computer Optics* 2023; 47 (4): 620-626. DOI: 10.18287/2412-6179-CO-1261.

## Introduction

Diabetes, as a metabolic disorder, had already been a worldwide health problem. According to the estimation of International Diabetes Federation, 537 million people had diabetes by the end of 2021, and this number will reach 643 million by 2030 [1]. Diabetes could cause various complications including the blindness, kidney failure, heart disease, stroke, and nontraumatic lower-limb amputations [2]. As a complication in eyes, diabetic retinopathy (DR) is the leading cause of blindness in the working-aged adults [3]. The systematic screening for diabetic patients was recognized as a primary method to prevent or delay the onset of DR [4]. The ophthalmic tools in clinic for diagnosing DR include ophthalmoscopy, fundus photography (FP), fundus fluorescein angiography (FFA), optical coherence tomography (OCT), and optical coherence tomography-based angiography (OCTA) [5–6]. Of those tools, FFA was recognized as the gold standard to

stage DR by evaluating vascular alterations in the retina [7]. However, FFA is an invasive methodology with the allergic risk by injecting the fluorescent dye into the bloodstream. While OCTA can generate the maps of the microvasculature of the retina in a non-invasive manner, it was recognized as a novel and promising tool to assist the doctors to diagnose the DR and avoid the allergic risk of the injection of the fluorescent dye [8].

In the diagnosis of DR, various features were extracted from OCTA images to describe the vasculature alterations in the retina. The typical features included the microaneurysms (MAs), foveal avascular zone (FAZ) parameters, vessel density (VD), and fractal dimension (FD). The MAs could be found in both the superficial capillary plexus (SCP) and DCP within the retina by using OCTA while it is not possible with FA [9]. And the significant correlation between DR stage and percentage of MAs morphology in OCTA and between MAs morphology and the presence of leakage in FA were also found

[10]. Furthermore, MAs in diabetic patients without clinical DR were observed by using OCTA [11]. As an avascular zone in the retina, the FAZ played an important role in the diagnosis of DR. The FAZ parameters included the FAZ area, FAZ axis ratio, horizontal and vertical FAZ radius, angle of maximum FAZ diameter and other parameters [12]. For example, the mean FAZ area in SCP was significantly increasing in DR group when comparing to normal healthy group [13–14]. The VD extracted from OCTA images can be used as an indicator to differentiate the diabetic patients with DR from normal healthy subjects. Studies showed that the mean VD in diabetic patients with the DR decreased when comparing to normal healthy subjects [15–17]. The FD is used to denote the vasculature changes in DR by describing the complexity of the distribution of vasculature in OCTA images [18–20]. Though those typical features could be used in the diagnosis of DR, the extractions from OCTA images needed to perform appropriate image processing techniques which might be a complicated and time-consuming procedure.

According to the previous study with OCT, the intensity parameters showed the diagnostic power in the diagnosis of DR [21]. In this study, we aimed to determine the diagnostic abilities of intensity parameters extracted from OCTA images in the diagnosis of DR.

## 1. Methodology

### 1.1. Ethic

This study was carried out in the ophthalmic center at Ningbo First Hospital and was approved by the Institutional Review Board of Ningbo First Hospital. The tenets of the Declaration of Helsinki were followed in this study. A written informed consent was obtained from each participant, after all procedures were explained in detail.

### 1.2. Subjects

78 normal healthy eyes, 10 diabetic eyes with mild NPDR, and 10 diabetic eyes with moderate NPDR were employed in this study. The statistical information about the subjects were listed in Tab. 1. All diabetic patients had the type 2 diabetes mellitus.

Tab. 1. Statistical information of the subjects

Group	The number of subjects (Female/Male)	The number of eyes	Age (mean±SD)
Control (healthy group)	42 (33/9)	78	46.55±13.55
Mild NPDR	6 (3/3)	10	62.17±13.99
Moderate NPDR	8 (3/5)	10	62.63±10.45

The inclusion criteria were listed as follows:

- 1) Confirmed diagnosis of the type 2 diabetes mellitus;
- 2) best corrected visual acuity was equal to or greater than 0.6;
- 3) intraocular pressure was in the normal range;
- 4) no severe heart, liver, lung and kidney diseases;
- 5) no history of eye trauma;

6) no history of eye surgery.

The main exclusion criteria were listed as follows:

- 1) Unable to complete the examination;
- 2) the subjects with any retinal or ocular disease such as glaucoma, vitreomacular diseases, and age-related macular degeneration etc.

The diabetic patients with DR were staged according to the Early Treatment Diabetic Retinopathy Study (ETDRS). The diabetic patient with mild NPDR is  $\geq 1$  microaneurysm with no other findings. While the diabetic patient with moderate NPDR has one of the following signs:  $\geq 20$  intraretinal hemorrhages in 1–3 quadrants, or venous beading in no more than 1 quadrant, or presence of mild intraretinal microvascular abnormalities (IRMAs) in no more than 1 quadrant [22].

### 1.3. Study protocol

The full ophthalmological examinations including slit lamp examination, fundus photography, intraocular pressure, and OCTA imaging were performed on each subject. Two experienced readers - Dr. Lin and Dr. Yan independently evaluated all subjects to stage DR based on the above examinations' results. If their evaluations were different, the retina specialist - Dr. Chen would make the final decision to stage DR.

### 1.4. Image acquisition

The OCTA images were collected at Ningbo First Hospital by using a commercial Heidelberg Engineering SPECTRALIS OCTA device. This device has an 870 nm-centered light source with the 50 nm bandwidth. A full-spectrum probabilistic approach was used in the Spectralis OCTA algorithm which it could generate the map in 85000 A-scans per second with the high contrast appearance. The 3×3 mm OCTA images of nerve fiber layer vascular plexus (NFLVP), superficial vascular plexus (SVP), intermediate capillary plexus (ICP) and deep capillary plexus (DCP) were generated for each eye [23].

### 1.5. Samples of OCTA image

The samples of OCTA DCP images of a normal healthy eye (left image) and a diabetic eye with mild NPDR (right image) were showed in Fig. 1. Compared to the normal healthy eye, the microvasculature of the diabetic eye with mild NPDR showed the irregularity and abnormalities that were labeled in the red boxes. It may suggest the retinal vascular occlusion and nonperfusion.

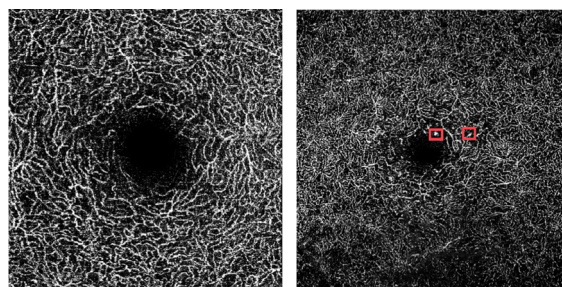


Fig. 1. Example of OCTA DCP images of a normal healthy eye and a diabetic eye with mild NPDR

1.6. Sectors in parafoveal zone

According to ETDRS, the sectors, namely, superior (S), temporal (T), inferior (I), nasal (N) in the parafoveal zone were segmented. Fig. 2 showed the sectors in OS and OD eyes. The diameter of the inner ring is 1 mm. The diameter of the outer ring is 3 mm.

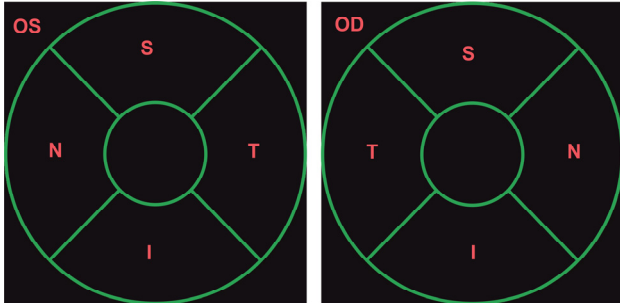


Fig. 2. Example of sectors of OS's (left eye) and OD's (right eye) OCTA images (3×3 mm) with an inner ring of 1mm diameter and an outer ring of 3mm diameter (abbreviation: S – superior sector, T – temporal sector, I – inferior sector, N – nasal sector)

1.7. Intensity parameters

Quantitative features in parafoveal zone such as thickness and FD with OCT [21, 24], and VD with OCTA [25] showed the diagnostic power to stage DR. In this study, the intensity parameters including the mean, median, variance, skewness, and kurtosis of intensities in sectors were calculated and the diagnostic abilities of them were investigated. The equations of the intensity parameters were listed in Tab. 2.

Tab. 2. Equations of intensity parameters

Intensity Parameters	Equation
Mean	$\bar{I} = \frac{\sum_{k=1}^N I_k}{N}$
Median	When the total number of pixels in region of interest (ROI) is an odd number, $Median = \left(\frac{N+1}{2}\right)^{th} I$ When the total number of pixels in ROI is an even number, $Median = \left[\left(\frac{N}{2}\right)^{th} I + \left(\frac{N+1}{2}\right)^{th} I\right]$
Variance	$Variance = \frac{\sum_{k=1}^N (I_k - \bar{I})^2}{N - 1}$
Skewness	$Skewness = \frac{\frac{1}{N} \sum_{k=1}^N (I_k - \bar{I})^3}{\left[\frac{1}{N} \sum_{k=1}^N (I_k - \bar{I})^2\right]^{3/2}}$
Kurtosis	$Kurtosis = \frac{\frac{1}{N} \sum_{k=1}^N (I_k - \bar{I})^4}{\left[\frac{1}{N} \sum_{k=1}^N (I_k - \bar{I})^2\right]^2}$

1.8. Study design

In order to find the reliable intensity parameters in sectors that were not affected by the factor of aging, the comparisons were performed among the normal healthy subjects to find the intensity parameters in sectors. The 41 normal healthy subjects were divided into 5 subgroups which their information was listed in Tab. 3. Only one normal healthy subject was not included since his age was over 70 years that was not in the range of 20 to 69.

Tab. 3. The statistical information of normal healthy subgroups

№	Age range	The number of subjects (Female/Male)	The number of eyes	Age (years)
G1	20~29	5 (4/1)	9	24.60±3.78
G2	30~39	10 (5/5)	19	35.10±2.60
G3	40~49	8 (10/0)	16	45.00±2.67
G4	50~59	11 (9/2)	20	54.64±3.26
G5	60~69	7 (10/0)	13	64.14±2.27

After the specific intensity parameters in sectors which did not show the statistically significant differences among normal healthy subgroups were found, the comparisons were performed between diabetic patients in early stages of DR and normal healthy subjects to check their diagnostic power in the early detection of DR.

1.9. Statistical analysis

The Student's t-test was used to find the differences between study groups. A p value less than 0.05 was considered statistically significant. The receiver operating characteristic (ROC) analysis was used to determine the discriminating power by calculating the area under the ROC curve (AUROC). An AUROC equal to 1.0 indicates perfect discriminative capacity, while an AUROC less than 0.5 indicates lack of discriminative capacity. The above two statistical analyses were done with IBM SPSS software, version 26.

2. Results

The specific sectors where the intensity parameters did not show the significant differences among the normal healthy subgroups were listed in Tab. 4. The values of intensity parameters of normal healthy subgroups and the p value of the comparisons between normal healthy subgroups were provided in the supplemental material.

The results of intensity parameters that showed a strong diagnostic power (AUROC ≥ 0.80, and sensitivity ≥ 0.80, and specificity ≥ 0.80) in the diagnosis of DR were listed in Tab. 5. Two comparisons were performed with the ROC analyses between diabetic patients with the early stages of DR (mild NPDR and moderate NPDR) and the normal healthy subjects. The area under ROC (AUROC) curves, asymptotic 95 % CI, cutoff point, sensitivity and specificity were calculated [26, 27]. The ROC curves were showed in Fig. 3 – 5. The values of intensity parameters of study groups and the p values of the comparisons were provided in the supplemental material.

Tab. 4. List of sectors where the intensity parameters did not show significant differences among normal healthy subgroups

Parameter	NFLVP	SVP	ICP	DCP
Mean	T, I, N	T, I, N	S, T, I	S, T, N
Median	S, T, I, N	T, I	T, I	S, T, I, N
Variance	I, N	I, N	S, T, I	S, T
Skewness	I, N	T	T, I	T, N
Kurtosis	I, N	T	S, T, I, N	T, N

Abbreviation: NFLVP – nerve fiber layer vascular plexus, SVP – superficial vascular plexus, ICP – intermediate capillary plexus, DCP – deep capillary plexus; S – superior sector, N – nasal sector, I – inferior sector, T – temporal sector.

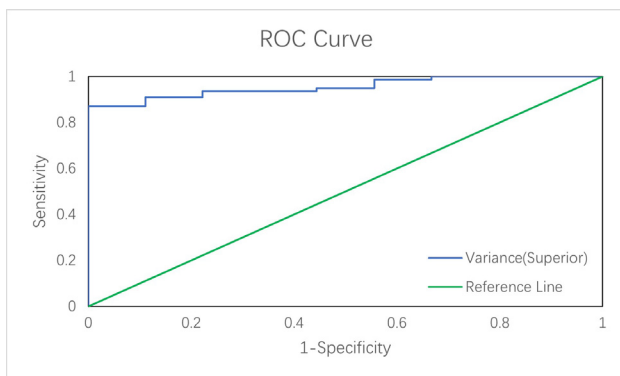


Fig. 3. The ROC curve of the variance of intensities in superior sector in ICP when comparing mild NPDR group to normal health group

Our results showed that the variance of intensities in superior sector in ICP achieved the highest AUROC value of 0.954 with the sensitivity of 0.872 and the specificity of 1.000 when comparing the diabetic patients with the mild

NPDR to normal healthy subjects. The mean intensity in superior sector in ICP achieved the second highest AUROC value of 0.947 with the sensitivity of 0.897 and the specificity of 0.900 when comparing the diabetic patients with the moderate NPDR to normal healthy subjects.

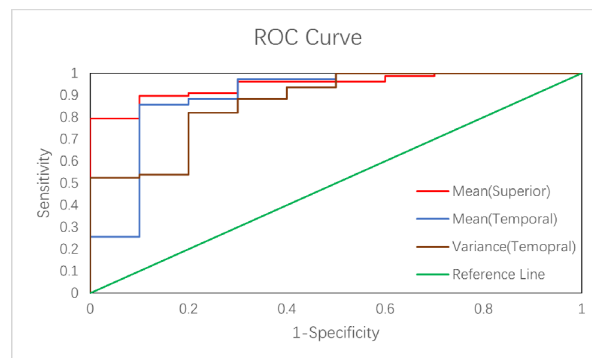


Fig. 4. The ROC curve of the mean in superior and temporal sectors and the variance in temporal sector in ICP when comparing moderate NPDR group to normal health group

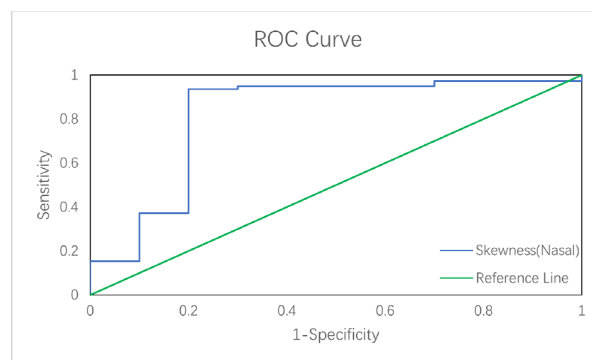


Fig. 5. The ROC curve of the skewness of intensities in nasal sector in NFLVP when comparing moderate NPDR group to normal health group

Tab. 5. The lists of the intensity parameters in sectors which showed the significant differences ( $p < 0.05$ ) between the DR groups and normal healthy group with the high AUROC ( $\geq 0.800$ ), sensitivity ( $\geq 0.800$ ), and specificity ( $\geq 0.800$ )

Comparison	Layer	Parameter	Sector	Area	Std error	Asymptotic sig	Asymptotic 95% CI		Cutoff point	Sensitivity	Specificity
							Lower bound	Upper bound			
Mild NPDR vs. Normal	ICP	Variance	S	0.954	0.022	0.000	0.911	0.998	786.331	0.872	1.000
Moderate NPDR vs. Normal	NFLVP	Skewness	N	0.818	0.092	0.001	0.638	0.998	2.980	0.936	0.800
	ICP	Mean	S	0.947	0.026	0.000	0.897	0.998	13.072	0.897	0.900
			T	0.895	0.070	0.000	0.757	1.000	14.395	0.859	0.900
		Variance	T	0.871	0.060	0.000	0.753	0.988	943.165	0.821	0.800

Abbreviation: NFLVP – nerve fiber layer vascular plexus, ICP – intermediate capillary plexus; S – superior sector, T – temporal sector, I – inferior sector, N – nasal sector, NPDR – n

### 3. Discussion and conclusion

DR, as a microvasculature disease in eyes, is the leading cause of blindness in working-aged adults around the world. The early detection of DR could help doctors treat this disease effectively and then help patients to prevent the visual loss. Since OCTA can map the microvascula-

ture in the retina, the information extracted from OCTA images may show the diagnostic ability to represent the vasculature alterations in the retina. Though the typical features such as MAs, VD, and FD may be used as indicators in the early detection of DR, it may need the complicated techniques and multiple steps to process the OCTA images and therefore it could be time-consuming. Our

study provided a different method to differentiate the early stages of DR by extracting the intensity parameters that did not need the complicated calculations and image processing techniques. The high AUROC value of the mean and variance of intensities in superior sector in ICP demonstrated that the intensity parameters directly extracted from OCTA images showed the strong diagnostic power to detect the diabetic patients with the mild/moderate NPDR. Furthermore, our study demonstrated that the changes of intensity parameters may reveal the vasculature alterations in diabetic patients with DR. OCTA is based on the concept that in a static eye the only moving structure in the fundus of the eye is blood flowing through the vessel [28]. And in OCTA images, the intensities of blood flows had the higher values than the intensities of static surrounding tissue.

The small mean intensity might represent a small number of pixels with the high intensity values which were occupied by the blood vessels. Therefore, the mean intensity may play a similar role to the VD in the diagnosis of DR since the VD is calculated as the percent area occupied by flowing blood vessels. Studies showed that the parafoveal VD decreased in diabetic eyes with DR when comparing to normal healthy eyes [29], which was consistent to our finding about the mean intensity. The variance is a measure of variability, which is calculated by taking the average of squared deviations from the mean value. The smaller variance means the less scattered intensity distribution in images, which also means the more clustered low or high values of intensity distribution in images. It could be due to the MAs showing in ICP in diabetic eyes with DR [30], which could generate the more areas with the higher intensities in OCTA images. Our results indicated that most of significant changes of intensity parameters in DR happened in the ICP. The ICP is located in the inner plexiform layer (IPL) containing synapses between bipolar and ganglion cells as well as amacrine cells [30–31]. The vascular endothelial growth factor (VEGF) signaling in amacrine cells plays a key role in regulating the development and capillary density in ICP [32], which cause vasculature alterations resulting in the changes of intensity parameters.

There are some limitations of our study. First, the sample sizes of the diabetic groups were limited. Second, OCTA images were obtained in 3×3mm, which included the FAZ and parafoveal zone only. The future study needs to obtain a larger number of subjects and a larger size of OCTA image.

In summary, our study demonstrated that the mean and variance of intensity in specific sectors showed strong diagnostic abilities in the early detection of DR. Compared to the common features, our study presented a relatively simple method to differentiate the diabetic patients in early stages from normal healthy subjects by calculating the intensity parameters from OCTA images.

### Acknowledgements

This study was supported by Zhejiang Provincial Natural Science Foundation (LY20H180009), Qianjiang Talent Plan (QJD1803009), Ningbo Science and Technology Service Industry Demonstration Project (2020F031), Zhejiang Provincial Traditional Chinese Medicine Science and Technology Project (2023ZL647), and Ministry of Science and Higher Education of the Russian Federation as part of the Program for increasing the competitiveness of Samara University among the world's leading research and educational centers for 2013–2020.

### References

- [1] International Diabetes Federation. IDF diabetes atlas, 10th ed. Brussels, Belgium: 2021. Source: <https://www.diabetesatlas.org>.
- [2] Selph S, Dana T, Bougatsos C, Blazina I, Patel H, Chou R. Screening for abnormal glucose and Type 2 diabetes mellitus: A systematic review to update the 2008 U.S. Preventive Services Task Force recommendation [Internet]. Report No 13-05190-EF-1. Rockville (MD): Agency for Healthcare Research and Quality (US); 2015. PMID: 25973510.
- [3] Cheung N, Mitchell P, Wong TY. Diabetic retinopathy. *Lancet* 2010; 376(9735): 124-136. doi: 10.1016/S0140-6736(09)62124-3.
- [4] Wong TY, Sabanayagam C. Strategies to tackle the global burden of diabetic retinopathy: From epidemiology to artificial intelligence. *Ophthalmologica* 2020; 243(1): 9-20. doi: 10.1159/000502387. PMID: 31408872.
- [5] Lee VS, Kingsley RM, Lee ET, Lu M, Russell D, Asal NR, Bradford RH Jr, Wilkinson CP. The diagnosis of diabetic retinopathy. *Ophthalmoscopy versus fundus photography*. *Ophthalmology* 1993; 100(10): 1504-1512. doi: 10.1016/s0161-6420(93)31449-1. PMID: 8414411.
- [6] Enders C, Baeuerle F, Lang GE, Dreyhaupt J, Lang GK, Loidl M, Werner JU. Comparison between findings in optical coherence tomography angiography and in fluorescein angiography in patients with diabetic retinopathy. *Ophthalmologica* 2020; 243(1): 21-26. DOI: 10.1159/000499114. PMID: 31137028.
- [7] de Barros Garcia JMB, Isaac DLC, Avila M. Diabetic retinopathy and OCT angiography: clinical findings and future perspectives. *Int J Retina Vitreous* 2017; 3: 14. DOI: 10.1186/s40942-017-0062-2. PMID: 28293432. PMCID: PMC5346852.
- [8] Corcóstegui B, Durán S, González-Albarrán MO, et al. Update on diagnosis and treatment of diabetic retinopathy: A consensus guideline of the working group of ocular health (Spanish Society of Diabetes and Spanish Vitreous and Retina Society). *J Ophthalmol* 2017; 2017: 8234186.
- [9] Ishibazawa A, Nagaoka T, Takahashi A, Omae T, Tani T, Sogawa K, Yokota H, Yoshida A. Optical coherence tomography angiography in diabetic retinopathy: A prospective pilot study. *Am J Ophthalmol* 2015; 160(1): 35-44.e1. DOI: 10.1016/j.ajo.2015.04.021. PMID: 25896459.
- [10] Fukuda Y, Nakao S, Kaizu Y, Arima M, Shimokawa S, Wada I, Yamaguchi M, Takeda A, Sonoda KH. Morphology and fluorescein leakage in diabetic retinal microaneurysms: a study using multiple en face OCT angiography image averaging. *Graefes Arch Clin Exp Ophthalmol* 2022; 260(11): 3517-3523. DOI: 10.1007/s00417-022-05713-7. PMID: 35665851.



- [11] Thompson IA, Durrani AK, Patel S. Optical coherence tomography angiography characteristics in diabetic patients without clinical diabetic retinopathy. *Eye (Lond)* 2019; 33(4): 648-652. DOI: 10.1038/s41433-018-0286-x. PMID: 30510234. PMCID: PMC6461750.
- [12] Gildea D. The diagnostic value of optical coherence tomography angiography in diabetic retinopathy: a systematic review. *Int Ophthalmol* 2019; 39(10): 2413-2433. DOI: 10.1007/s10792-018-1034-8. PMID: 30382465.
- [13] Takase N, Nozaki M, Kato A, Ozeki H, Yoshida M, Ogura Y. Enlargement of foveal avascular zone in diabetic eyes evaluated by en face optical coherence tomography angiography. *Retina* 2015; 35(11): 2377-2383. DOI: 10.1097/IAE.0000000000000849. PMID: 26457396.
- [14] Al-Sheikh M, Akil H, Pfau M, Sadda SR. Swept-source OCT angiography imaging of the foveal avascular zone and macular capillary network density in diabetic retinopathy. *Invest Ophthalmol Vis Sci* 2016; 57(8): 3907-3913. DOI: 10.1167/iovs.16-19570. PMID: 27472076.
- [15] Ragkousis A, Kozobolis V, Kabanarou S, Bontzos G, Mangouritsas G, Heliopoulos I, Chatziralli I. Vessel density around foveal avascular zone as a potential imaging biomarker for detecting preclinical diabetic retinopathy: An optical coherence tomography angiography study. *Semin Ophthalmol* 2020; 35(5-6): 316-323. DOI: 10.1080/08820538.2020.1845386. PMID: 33258720.
- [16] Xie N, Tan Y, Liu S, Xie Y, Shuai S, Wang W, Huang W. Macular vessel density in diabetes and diabetic retinopathy with swept-source optical coherence tomography angiography. *Graefes Arch Clin Exp Ophthalmol* 2020; 258(12): 2671-2679. DOI: 10.1007/s00417-020-04832-3. PMID: 32661699.
- [17] Lavia C, Couturier A, Erginay A, Dupas B, Tadayoni R, Gaudric A. Reduced vessel density in the superficial and deep plexuses in diabetic retinopathy is associated with structural changes in corresponding retinal layers. *PLoS One* 2019; 14(7): e0219164. DOI: 10.1371/journal.pone.0219164. PMID: 31318880. PMCID: PMC6638849.
- [18] Zahid S, Dolz-Marco R, Freund KB, Balaratnasingam C, Dansingani K, Gilani F, Mehta N, Young E, Klifto MR, Chae B, Yannuzzi LA, Young JA. Fractal dimensional analysis of optical coherence tomography angiography in eyes with diabetic retinopathy. *Invest Ophthalmol Vis Sci* 2016; 57(11): 4940-4947. DOI: 10.1167/iovs.16-19656. PMID: 27654421.
- [19] Chen Q, Ma Q, Wu C, Tan F, Chen F, Wu Q, Zhou R, Zhuang X, Lu F, Qu J, Shen M. Macular vascular fractal dimension in the deep capillary layer as an early indicator of microvascular loss for retinopathy in type 2 diabetic patients. *Invest Ophthalmol Vis Sci* 2017; 58(9): 3785-3794. DOI: 10.1167/iovs.17-21461. PMID: 28744552.
- [20] Sun Z, Tang F, Wong R, Lok J, Szeto SKH, Chan JCK, Chan CKM, Tham CC, Ng DS, Cheung CY. OCT angiography metrics predict progression of diabetic retinopathy and development of diabetic macular edema: a prospective study. *Ophthalmology* 2019; 126(12): 1675-1684. DOI: 10.1016/j.ophtha.2019.06.016. Erratum in: *Ophthalmology* 2020; 127(12): 1777. PMID: 31358386.
- [21] Gao W, Tátrai E, Ólvedy V, Varga B, Laurik L, Somogyi A, Somfai G, DeBuc D. Investigation of changes in thickness and reflectivity from layered retinal structures of healthy and diabetic eyes with optical coherence tomography. *J Biomed Sci Eng* 2011; 4: 657-665. DOI: 10.4236/jbise.2011.410082.
- [22] Wilkinson CP, Ferris FL 3rd, Klein RE, et al. Proposed international clinical diabetic retinopathy and diabetic macular edema disease severity scales. *Ophthalmology* 2003; 110(9): 1677-1682. DOI:10.1016/S0161-6420(03)00475-5.
- [23] Rocholz R, Teussink MM, Dolz-Marco R, et al. SPECTRALIS optical coherence tomography angiography (OCTA): principles and clinical applications. Heidelberg, Germany: Heidelberg Engineering Academy; 2018. Source: [https://www.heidelbergengineering.com/media/e-learning/Totara/Dateien/pdf-tutorials/210111-001\\_SPECTRALIS%20OCTA%20-%20Principles%20and%20Clinical%20Applications\\_EN.pdf](https://www.heidelbergengineering.com/media/e-learning/Totara/Dateien/pdf-tutorials/210111-001_SPECTRALIS%20OCTA%20-%20Principles%20and%20Clinical%20Applications_EN.pdf).
- [24] Gao W, DeBuc DC, Zakharov VP, et al. Two-dimensional fractal analysis of retinal tissue of healthy and diabetic eyes with optical coherence tomography. *J Biomed Photonics Eng* 2016; 2: 040302.
- [25] Mastropasqua R, Toto L, Mastropasqua A, Aloia R, De Nicola C, Mattei PA, Di Marzio G, Di Nicola M, Di Antonio L. Foveal avascular zone area and parafoveal vessel density measurements in different stages of diabetic retinopathy by optical coherence tomography angiography. *Int J Ophthalmol* 2017; 10(10): 1545-1551. DOI: 10.18240/ijo.2017.10.11. PMID: 29062774. PMCID: PMC5638976.
- [26] Hajian-Tilaki K. Receiver operating characteristic (ROC) curve analysis for medical diagnostic test evaluation. *Caspian J Intern Med* 2013; 4(2): 627-635. PMID: 24009950. PMCID: PMC3755824.
- [27] Unal I. Defining an optimal cut-point value in ROC analysis: An alternative approach. *Comput Math Methods Med* 2017; 2017: 3762651. DOI: 10.1155/2017/3762651. PMID: 28642804. PMCID: PMC5470053.
- [28] Coscas G, Lupidi M, Coscas F. Heidelberg spectralis optical coherence tomography angiography: Technical aspects. *Dev Ophthalmol* 2016; 56: 1-5. DOI: 10.1159/000442768. PMID: 27022921.
- [29] Agemy SA, Scripsema NK, Shah CM, Chui T, Garcia PM, Lee JG, Gentile RC, Hsiao YS, Zhou Q, Ko T, Rosen RB. Retinal vascular perfusion density mapping using optical coherence tomography angiography in normals and diabetic retinopathy patients. *Retina* 2015; 35(11): 2353-2363. DOI: 10.1097/IAE.0000000000000862. PMID: 26465617.
- [30] Park JJ, Soetikno BT, Fawzi AA. Characterization of the middle capillary plexus using optical coherence tomography angiography in healthy and diabetic eyes. *Retina* 2016; 36(11): 2039-2050. DOI: 10.1097/IAE.0000000000001077. PMID: 27205895. PMCID: PMC5077697.
- [31] Tan PE, Yu PK, Balaratnasingam C, Cringle SJ, Morgan WH, McAllister IL, Yu DY. Quantitative confocal imaging of the retinal microvasculature in the human retina. *Invest Ophthalmol Vis Sci* 2012; 53(9): 5728-5736. DOI: 10.1167/iovs.12-10017. PMID: 22836777.
- [32] Provis JM. Development of the primate retinal vasculature. *Prog Retin Eye Res* 2001; 20(6): 799-821. DOI: 10.1016/s1350-9462(01)00012-x. PMID: 11587918.

---

### *Authors' information*

**Jiayi Hou**, Female, DoB: 2002-02-03, Research Assistant, Senior college student in School of Safety Engineering, Ningbo University of Technology.

**Hongtao Shi**, Male, DoB: 2002-11-16, Research Assistant, Senior college student in school of Safety Engineering, Ningbo University of Technology.

**Wei Gao** (obtained PhD degree in Biomedical Engineering from University of Miami in Miami in 2012), DoB: 1980-02-6, Assistant Professor at School of Computer Science, Ningbo University of Technology.  
E-mail: [gwei@nbut.edu.cn](mailto:gwei@nbut.edu.cn).

**Pengyao Lin** (obtained Master degree of Medicine from Capital Medical University in Beijing in 2010), Male, DoB: 1987-09-25, Attending Physician at Ningbo First Hospital.

**Bo Li** (obtained Bachelor degree of Medicine from Zhejiang University in Hangzhou in 1986), Female, DoB: 1963-01-29, Director Physician at Ningbo First Hospital.

**Yan Shi** (obtained Master degree of Medicine from Nanjing University in Nanjing in 2008), Male, DoB: 1982-12-20, Assistant Director Physician at Ningbo First Hospital.

**Irina A. Matveeva**, born in 1995, is a postgraduate student of Laser and Biotechnical Systems department, Samara National Research University. In 2017 she graduated from a bachelor's degree, in 2019 from a master's degree in "Biotechnical Systems and Technologies" at Samara National Research University. Research interests: biophotonics, Raman spectroscopy, mathematical modeling. E-mail: [m-irene-a@yandex.ru](mailto:m-irene-a@yandex.ru).

**Valery P. Zakharov** (b 1954) received his PhD (1984) in Theoretical Physics from Bogolyubov Institute for Theoretical Physics, Kiev, Ukraine, and his DSc (1999) in Optics from SSAU. Currently, he is a professor and holds the Laser and Biotechnical Systems chair. He is a head of the «Photonics» research laboratory of SSAU. His research interests include biophotonics, biomedical optics, spectroscopy, laser physics and techniques, medical lasers.  
E-mail: [zakharov@ssau.ru](mailto:zakharov@ssau.ru).

**Ivan A. Bratchenko** (b. 1985) received MSc in Applied Mathematics and Physics from Samara State Aerospace University (SSAU) in 2009, received a PhD in 2012. Now he is an assistant professor of Laser and Biotechnical Systems department of SSAU and a leading researcher of the «Photonics» laboratory of SSAU. His research interests include biophotonics, optics and spectroscopy, mathematical modeling. E-mail: [iabratchenko@gmail.com](mailto:iabratchenko@gmail.com).

---

*Code of State Categories Scientific and Technical Information (in Russian – GRNTI): 29.31.29*  
*Received: December 8, 2022. Final version: April 11, 2023.*

---